PAPER

Automated analysis of natural variations in isotopes of silicon by the thermal decomposition of BaSiF$_6$

Mark A. Brzezinski, [ID] *[ab] Stephen F. Rablen,[c] Janice L. Jones,[ID][a] Ivia Closset[ad] and Julien T. Middleton[a]

The performance of a new inlet system, the Nu Sil, for the automated determination of the isotopic abundances of silicon in SiF$_4$ gas generated from the thermal decomposition of BaSiF$_6$ is reported. The inlet system is coupled to an isotope ratio mass spectrometer through a conventional dual inlet system. The method uses straightforward and proven sample preparation chemistry that is suitable for converting the silicon in biogenic and lithogenic solids, or that dissolved in fresh or salt waters, to BaSiF$_6$. Yields of silicon tetrafluoride are 99.8 $\pm$ 0.16%. δ^{30}Si values obtained with the method for a variety of natural and synthetic materials agree with published values to better than 0.05‰. External long-term average δ^{30}Si values of the solid standard NBS28, the secondary standards Big Batch and diatomite, and the reference seawater ALOHA$_{1000}$ are all within 0.03‰ of their respective consensus values. Typical loading of BaSiF$_6$ represents 10 to 40 µg of Si. The analytical rate is 30 unattended analyses daily.

1 Introduction

Silicon is the seventh most abundant element in the universe by both mass and mole fraction and it is the second most abundant element in the Earth's crust, after oxygen. The three stable isotopes of silicon have mass 28, 29 and 30 with relative abundances of 92.229, 4.683, and 3.087 atom%, respectively.[1] Natural variations in the relative abundance of stable isotopes of silicon in various materials are increasingly being employed as an investigative tool in biology,[2–8] in cosmology and planetary science[9–14] and in geochemistry.[15–22] The measurement of isotopes of Si is challenging as the extent of natural variation can be small, one to a few parts per thousand,[23] necessitating analytical methods with high accuracy and high precision.

The most common instruments presently employed in Si isotope measurement are multi-collector inductively coupled plasma mass spectrometers (MC-ICPMS).[24] These instruments and associated preparatory chemistry can analyze small samples and have reasonable analytical throughput, but they require frequent, if not daily, tuning and they are sensitive to matrix effects, mass discrimination and temporal drift in isotope ratios. Less common are methods employing isotope ratio mass spectrometers (IRMS). For IRMS, the analyte gas, SiF$_4$, is prepared either by high temperature fluorination by the reaction of Si compounds with F$_2$ (ref. 10 and 25) or BrF$_5$,[26]

through the acid decomposition of Cs$_2$SiF$_6$ (ref. 27) or through the thermal decomposition of BaSiF$_6$.[28,29] Fluorination with F$_2$ or BrF$_5$ has the advantage of allowing the simultaneous determination of silicon and oxygen isotope values in silicates.[10,30] IRMS methods are largely free of matrix effects and mass discrimination is less than in MC-ICPMS, but they often employ hazardous chemicals and typically require larger samples than do those employing MC-ICPMS. They have historically required custom-built vacuum lines (fluorination) or customized inlet systems (acid decomposition), hampering adoption.

Here we evaluate a new commercial inlet system, the Nu Sil, manufactured by Nu Instruments Ltd, that automates the analysis of Si isotopes using IRMS with SiF$_4$ generated through the thermal decomposition of BaSiF$_6$ according to:

$$\text{BaSiF}_6 \text{ (s)} \rightarrow \text{SiF}_4 \text{ (g)} + \text{BaF}_2 \text{ (s)} \tag{1}$$

The SiF$_4$ is ionized *via* electron bombardment producing SiF$_3^+$ ions as the main fragment. As fluorine consists of a single isotope of mass nineteen, ^{28}SiF$_3^+$, ^{29}SiF$_3^+$ and ^{30}SiF$_3^+$ produce ion beams at m/z 85, 86 and 87, respectively. The thermal decomposition of BaSiF$_6$ was among the first methods employed to measure stable isotopes of Si in natural materials.[31,32] More recently, it has been employed to make highly accurate absolute Si isotope abundance measurements in support of refining the Avogadro constant.[28,33,34] The requisite sample preparation chemistry and the thermal decomposition of the compound are both known to not fractionate isotopes of Si;[28] however, BaSiF$_6$ methods have been criticized for being slow and for requiring large sample mass.[35] The new instrumentation and sample preparation methods presented here are

[a]*Marine Science Institute, University of California Santa Barbara, Santa Barbara, CA, USA*

[b]*Department of Ecology Evolution and Marine Biology, University of California Santa Barbara, Santa Barbara, CA, USA*

[c]*Nu Instruments Ltd, PO Box 36, 2 New Star Road, Leicester, LE4 9JQ, UK*

[d]*Finnish Meteorological Institute, Helsinki, Uusimaa, Finland*

This journal is © The Royal Society of Chemistry 2025

J. Anal. At. Spectrom., 2025, **40**, 3495–3506 | **3495**

straightforward to implement, have relatively high sample throughput (30 unattended samples per day) and are capable of analyzing small samples (≥ 10 μg Si as $BaSiF_6$) with accuracy and precision comparable to MC-ICPMS.

2 Experimental

2.1 Construction of the Nu Sil inlet system

The method employs a new commercially available inlet system, the Nu Sil, which automates the decomposition of $BaSiF_6$ to produce SiF_4 gas that is analyzed by dual inlet IRMS. The Nu Sil is manufactured by Nu Instruments Ltd, Leicester, UK which is a subsidiary of AMETEK, Incorporated. The system is a modification of the company's Nu Carb device for the analysis of $\delta^{13}C$ and $\delta^{18}O$ isotope ratios in carbonates. The main modifications consist of replacing the acid dosing system of the Nu Carb with a miniature variable-temperature tube furnace mounted just below the attachment port for sample vials and the substitution of a bleed temperature optimized (BTO) silicone gasket in place of the Nu Carb's Viton® gasket that seals the sample vial to the sample vacuum port (Fig. 1 and 2).

The furnace is 1.5 cm long and is resistively heated with temperature feedback *via* a thermocouple inserted into the body of the furnace tube. A control circuit achieves temperatures from 100 to 600 °C to within 3 °C. The furnace is mounted so that the open central bore is aligned with the vertical axis of the shaft that lifts glass sample vials up to the sample inlet port (Fig. 1A). When a sample vial is raised through the inner bore of the tube furnace, the flat vial lip is pressed against a BTO seal and the lower half of the vial aligns with the center of the tube furnace with the upper 1.5 cm of the vial protruding above the top of the furnace (Fig. 1B). This configuration allows the $BaSiF_6$ that is located in the conical depression in the bottom of the vial to be heated to the reaction temperature of 590 °C without the lip of the vial exceeding the thermal tolerance of the BTO seal (∼400 °C). A lightweight sheet-metal heat shield protects the vacuum valves and the vial detection system that are positioned above the sample port from radiant heat (Fig. 1 and 2). Because sample vials are pushed entirely out of the carousel into the furnace tube, the sample carousel is modified from the Nu Carb design, being taller with chamfered vial receptacles to allow vials to relocate easily after sampling. All other hardware is unmodified from that on the Nu Carb.

The Nu Sil is connected to an unmodified Nu perspective IRMS equipped with a dual inlet. The preamplifiers on the Faraday collectors are equipped with gain resistors of 1 GΩ, 100 GΩ and 100 GΩ for measurement at m/z 85, 86 and 87,
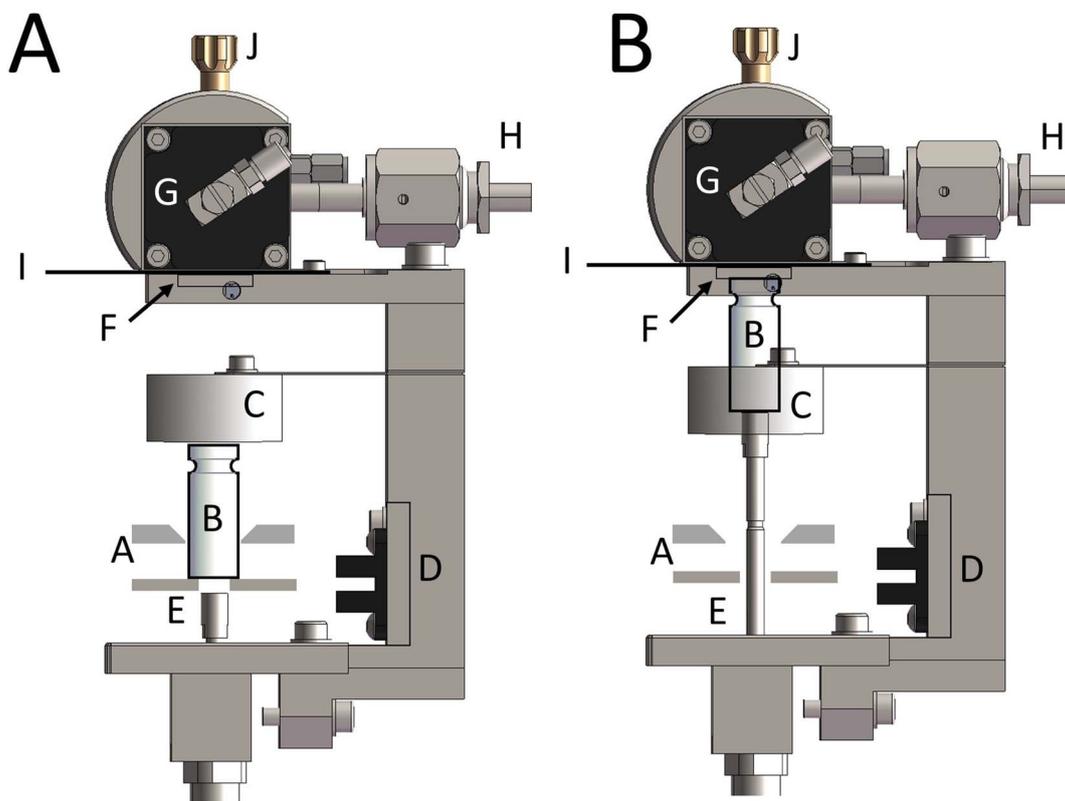
Fig. 1 Schematic showing a side view of the Nu Sil sample heater and valve block assembly shown as a photograph in Fig. 2. In A the sample carousel (A) rotates each sample vial (B) into position beneath the tube furnace (C) using the carousel optical alignment device (D). In B the lifting mechanism (E) raises the sample vial through the tube furnace (C) to position the sample within the furnace pressing the vial opening against the BTO seal on sample port (F). Evacuation is accomplished through valve block G that is connected to the CF PREP cold finger (not shown) through stainless tube H. A sheet metal heat shield (I) protects the valve block from radiant heat. A threaded plug (J) seals off a port formerly used for acid introduction the Nu Carb and can be opened to clean the internals of the sample port.

3496 | *J. Anal. At. Spectrom.*, 2025, **40**, 3495–3506

This journal is © The Royal Society of Chemistry 2025

Fig. 2 Photograph of the inside of the Nu Sil sample chamber showing components illustrated in Fig. 1: the sample carousel with samples vials (A & B), the Nu Sil heater (C), the heat shield (I), vacuum valves (G), cleaning port (J) and outlet to the CF PREP cold finger (H). Other components shown in Fig. 1 are obscured in the view shown.

respectively. The control software is customized to operate the Nu Sil and to execute a custom control sequence for valve and cold finger operation on the dual inlet and the Nu perspective IRMS as described in section 2.3.

2.2 Preparation of BaSiF$_6$

The method is amenable to the analysis of both aqueous and solid samples. To prepare aqueous samples as BaSiF$_6$, the Si is first concentrated by precipitation as triethylamine silicomolybdic acid by the addition of acidified triethylamine ammonium molybdate (TEA-moly).[27] The precipitate is recovered by filtration and combusted to produce solid SiO$_2$.[25] Solid samples that contain significant impurities are processed similarly after dissolution in HF or after high temperature fusion with NaOH flux in Teflon[36] or with Na$_2$CO$_3$ flux in platinum[37] to produce water-soluble sodium silicate, SiO$_2$: Na$_2$O. The TEA-moly procedure is not necessary for higher purity solid samples or solid standards.

Solid SiO$_2$ from the TEA-moly procedure or from naturally occurring solids is converted to BaSiF$_6$ as follows: up to 2.4 mg of SiO$_2$ is placed in a 5 mL polypropylene or polyethylene snap-cap centrifuge tube and 1 mL of 7.5 M HF is added to dissolve the sample and produce SiF$_6^-$ ions. (The final concentration of dissolved Si must be <40 mM to prevent Si volatilization[25]). After allowing 24 to 48 h for sample dissolution (24 for amorphous silica, 48 h for crystalline forms), 0.5 mL of 3 M CsCl is added to precipitate Cs$_2$SiF$_6$. After 12 hours, the precipitate is isolated by centrifugation and rinsed 3 times with ethanol. The final product is dried in the centrifuge tube at 65 °C. Conversion of Cs$_2$SiF$_6$ to BaSiF$_6$ takes advantage of the greater solubility of Cs$_2$SiF$_6$ (0.60 g per 100 mL H$_2$0) compared to BaSiF$_6$ (0.026 g 100 mL H$_2$0) whereby 2.4 mL of an aqueous solution that is 17 mM in BaCl and 2 mM in HF is added to the dry Cs$_2$SiF$_6$ to dissolve the Cs$_2$SiF$_6$ and precipitate BaSiF$_6$. After 24 h the BaSiF$_6$ is isolated by centrifugation, rinsed with alcohol and dried as described for Cs$_2$SiF$_6$. Samples are stored sealed in the centrifuge tubes at room temperature and are stable indefinitely.

2.3 Sample loading

A typical analysis involves loading 100 to 600 μg of BaSiF$_6$ into a glass sample vial (Fisher Scientific #13 622271 – 1.5 mL high recovery vial, crimp or snap top) using a Wiretrol II®, 1–5 μL

This journal is © The Royal Society of Chemistry 2025

J. Anal. At. Spectrom., 2025, **40**, 3495–3506 | **3497**

disposable micropipette. The Wiretrol consists of a narrow-bore glass tube fitted with a metal plunger of equal length that rides along the inner bore of the glass tube. The metal plunger has a plastic loop on one end that serves both as a handle for the user and as a stop between the metal plunger and glass tube. Several metal plungers were cut to different lengths to aid in loading samples of various predetermined sizes based on the distance from the end of the glass tube to the end of the shortened plunger. When fully inserted into the glass tube the shortened plunger creates a gap between itself and the end of the glass tube, thus setting the depth of sample that will fit in the tube with sample size dictated by the choice of plunger length. A modified Wiretrol is inserted in the $BaSiF_6$ pellet in the bottom of the centrifuge tube several times to pack the gap with the powder. The $BaSiF_6$ is ejected into a sample vial by one or two short strokes of the metal plunger. The glass tube is discarded and the metal plunger cleaned by wiping with a lint-free wipe wetted with ethanol before reuse. Sample vials containing $BaSiF_6$ are placed in the sample carousel and heated in a ventilated oven at 110 °C for at least 2 h to drive off moisture and any remnants of the mother liquid. The carousel and samples are transferred while hot to the Nu Sil sample chamber, which is maintained at 70 °C. Once in the Nu Sil, samples are analyzed sequentially.

2.4 Sample analysis

2.4.1 Filling the reference gas bellows. A schematic of the sample processing system of the Nu Sil and Nu perspective is depicted in Fig. 3. Prior to analyzing a carousel of samples, the reference bellows is filled with commercial SiF_4 (semiconductor grade, 99.999% SiF_4) that is stored in a small home-made stainless-steel cylinder (~5 L volume) at ~45 psi with the exit port consisting of three valves in series that are separated by ~2 cm of 6 mm OD stainless steel tubing. The last valve on the cylinder is attached at valve GB *via* an uncrimped capillary identical to those used on the Nu perspective. The three valves

allow an increasing volume of 45 psi gas to be used during the refill process as the reference gas is depleted over time. A tank of reference gas lasts for a several thousand samples.

The initial filling of an empty reference bellows from a full reference gas tank proceeds as follows: the refill capillary is pressurized behind valve GB (closed) by opening all 3 valves on the reference gas canister and waiting ~10 minutes for isotopic equilibrium. The lower 2 valves on the refill tank are closed so that SiF_4 is constrained to the volume of the refill capillary and the 2 cm piece of 6 mm OD tubing located between the last valve on the refill cylinder and the capillary. This reduced volume is necessary to slow the filling of the bellows so that the following manual fill sequence is manageable: first, the changeover valve is set to allow reference gas into the ionization source of the mass spectrometer. Then the reference bellows is expanded to 100%. With valves SP, GB and RM closed, valves RI, RP, RV and LV are opened to evacuate the reference bellows and the tubing between RM and GB under low vacuum for 3 minutes. Then LV is closed and HV opened to evacuate under high vacuum for another 3 minutes. Valves RF, RV and HV are then closed and LV opened. Then, while still actively pumping under low vacuum, valve GB is opened for 5 s to establish flow from the reference gas capillary after which valve RP is closed. Valves RF, RV and RM are opened and the signal intensity at m/z 85 is monitored. When the signal reaches ~1.9×10^{-9} amperes (~20% of signal saturation) valve GB is closed and the signal intensity at m/z 85 is allowed to stabilize for 3 minutes after which a reading of ~2.2×10^{-9} amperes at m/z 85 is typically reached. On subsequent refills of the bellows it is not necessary to evacuate the remaining SiF_4 from the bellows and valve RV can be closed during the initial evacuation of space between valves RF, RV and RI.

2.4.2 Nu perspective tuning. Following the refilling of the reference bellows, the ion beam peak shape is checked using the reference gas (Fig. 4). Adjustments are made to the ion source parameters and zoom optics of the Nu perspective as
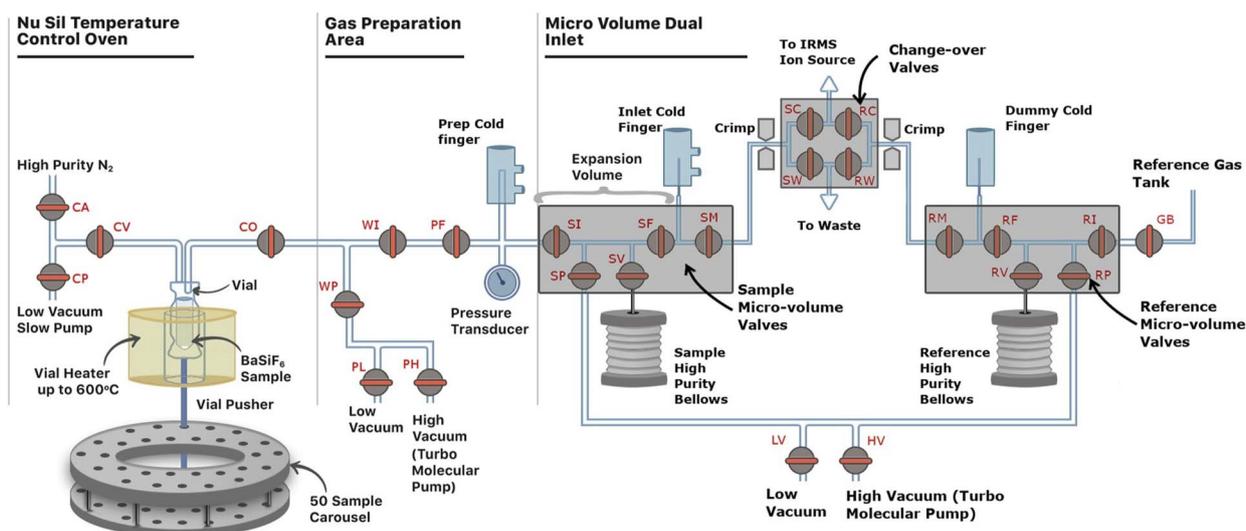

Fig. 3 The Nu Sil and Nu perspective gas handling systems. Valves are labeled following the labeling scheme in the Nu Sil software.
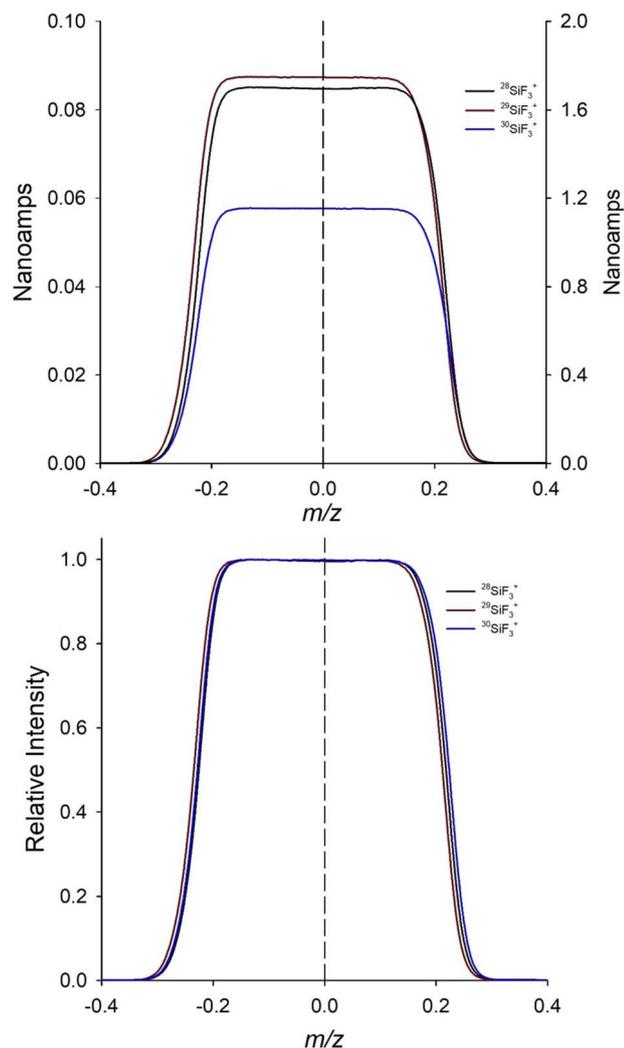
3498 | *J. Anal. At. Spectrom.*, 2025, **40**, 3495–3506

This journal is © The Royal Society of Chemistry 2025

Fig. 4 Peak shape obtained for SiF_3^+ ions at m/z 85, 86 and 87. Abscissa for all peaks is scaled to the center of each peak. (A) Raw peak intensity from the amplifiers on the Faraday cups in nanoamperes. (B) Peaks normalized relative to their maximum beam intensity.

needed. Daily adjustments are rare as peak shape and sensitivity are stable over days to weeks, but peak shape is checked before each analytical run.

2.4.3   Sample loading. Sample preparation begins with the lifting mechanism raising a vial up out of the sample carousel, through the tube furnace so that the open end of the vial is held pressed against the sample inlet port of the Nu Sil (Fig. 3). To establish vacuum, the vial is first "soft pumped" so as to not disturb the $BaSiF_6$ powder by opening valves CP and CV (CA & CO are closed) which evacuates the vial to 0.7 Pa slowly through one meter of 0.5 mm inner diameter PEEK tubing *via* a scroll pump. Then valves CP and CV are closed and the vial pumped by the scroll pump more rapidly to 0.1 Pa by opening valves CO, WP and PL for 30 s. The vial is then placed under high vacuum ($<1 \times 10^{-6}$ Pa) by closing valve PL and opening valve PH to a turbo molecular pump. The vial is heated to 250 °C under high vacuum for 20 minutes with valves PF and WI open so that the PREP cold finger is also evacuated.

2.4.4 SiF_4 generation and processing. SiF_4 is generated by first closing valve WP and PH to isolate the sample train from vacuum (Fig. 3). Valves CO, WI and PF remain open (valves SI and CV are closed) forming a direct path from the sample vial to the PREP cold finger. The sample temperature is raised from 250 °C to 590 °C as the PREP cold finger is cooled with liquid nitrogen to −180 °C to freeze down SiF_4 gas as it is generated. The reaction proceeds for 10 min from the time when the furnace temperature first reaches 580 °C. When the reaction is complete, solid BaF_2 remains in the bottom of the sample vial and all SiF_4 has been frozen into the PREP cold finger. Then non-condensable gases, if any, are pumped away at low vacuum by opening valve WP and PL until a vacuum of 0.1 Pa is reached and then under high vacuum for 60 seconds by closing PL and opening PH. The PREP cold finger with the frozen SiF_4 is then isolated by closing valve PF and the tube furnace is turned off. The PREP cold finger is then warmed to 15 °C to release the SiF_4 whereafter the gas pressure on the inlet pressure transducer is recorded as an indicator of sample size. At this point the generation of SiF_4 is complete and the SiF_4 is transferred to the dual inlet by cooling the INLET cold finger to −180 °C and opening valves SI and SF (valves SM, SV and SP are closed) for 3 minutes to freeze-transfer the SiF_4 to the INLET cold finger. Valves SI and SF are then closed to isolate the INLET cold finger which also serves as the microvolume of the sample side of the dual inlet system. The INLET cold finger is then heated to 15 °C to release the SiF_4 completing sample preparation.

Prior to isotopic analysis, the SiF_4 generation subsystem is prepared for the next sample. By this time the tube furnace has cooled to <150 °C and valve CO is closed and the sample vial is detached from the sample port by introducing high purity (99.998%) nitrogen gas by opening valves CA and CV to relieve vacuum. The sample vial lowered back into the sample carousel and valves CA and CV are then closed. The next sample vial is rotated into position and attached to the sample port, brought under vacuum and the prebake at 250 °C initiated as above. The PREP cold finger is heated to 100 °C under high vacuum with valves WP, WI, PF and CO open. After 30 s at 100 °C the cold finger is allowed to passively cool and evacuate during the rest of the sample prebake at 250 °C.

2.4.5   Isotopic analysis. Isotopic analysis proceeds by first accessing the signal strength produced by the sample gas. Valve SM is opened with the changeover valve set to allow sample gas to flow from the sample microvolume through the crimped capillary to the ionization source of the Nu perspective. If the signal intensity of any one of the ion beams, $^{28}SiF_3^+$, $^{29}SiF_3^+$, $^{30}SiF_3^+$ exceeds their respective amplifier limits, then valve SM is closed and SF is opened (SV, SI and SP remain closed) to expand the sample gas into a larger volume to reduce its pressure, and the signal is reassessed. Should further pressure reduction be required, the sample gas is 'chopped' before reassessment by closing valve SF and evacuating the space between valves SI, SP, SV and SF by opening SP (valve HV is open) for 200 s. Then valve SP is closed, and the remaining sample gas is expanded again by opening valve SF (SV remains closed during all inlet side operations unless the sample is large enough to utilize the bellows,

which is not routine). Once all sample beams are within amplifier limits, sample gas is contained between the capillary crimp and valve SF (valve SM is open) for samples that did not require expansion or chopping, while for expanded and chopped samples sample gas occupies the volume from the crimp to valve SI (valves SP and SM are closed).

Analysis of the sample begins with both the reference and sample gas streams directed to waste in the changeover valve. The changeover valve is then set to introduce reference gas into the ionization source, and a peak-centering routine is performed at m/z 85 to determine the magnet setting for measuring beam intensity at the center of the peaks. Then both the sample and reference gas streams are directed back to waste and the signal at m/z 85 is monitored every 7 s until its value has fallen by no more than 1×10^{-14} amperes between readings. The background ion beam intensities at m/z 85, 86 and 87 are then each measured for 8 s and the means of these readings are subsequently subtracted from all sample readings at each respective m/z. The reference-gas bellows is adjusted so that the reference gas ion beam intensity at m/z 85 matches that of the sample after which the bellows and sample beam intensities are typically within 1% or better of one another. Then the reference-valve configuration is set to match that of the sample's with valve RM open and RF is closed for samples that did not require expansion or chopping or with valves RM and RF open (valves RV, RI and RP are closed) for samples that were expanded or chopped. Sample and reference gas are now at the same pressure, confined to identical volumes and continuously pumped either to the ion source of the Nu perspective or to waste through matched crimped capillaries so that the sample and reference gas deplete at the same rate during sample analysis. Sample measurement proceeds using 8 sample/reference cycles of the changeover valve with each reading of the sample or reference gas lasting 20 s at 10 Hz.

When the analysis is complete the remaining sample gas is pumped to waste by opening valves SF and SP (PH is open). The INLET cold finger is heated to 100 °C for 30 s and the sample side of the dual inlet is pumped for 6 minutes at high vacuum. Total sample analysis time is 65–70 minutes depending on the time required for sample chopping and balancing sample and reference gas pressures. As preparation of the next sample begins before the previous sample is fully analyzed, the effective analytical throughout after the first sample averages 48 minutes to obtain the raw uncalibrated delta values for a sample.

2.5 Calibration

Samples are calibrated against the international standard NBS28 (RM8546) and the well-characterized secondary standards Big Batch and diatomite.[24,38] All three standards are routinely analyzed at the beginning and end of each analytical run and the results used to calculate sample isotope values using a multipoint calibration method.[39] For calibration, the measured $\delta^{30}Si$ values for all three reference materials ($\delta^{30}Si_{measured}$) are regressed against their consensus $\delta^{30}Si$ values with NSB = 0‰, Big Batch = $-10.48‰$ and diatomite = $+1.26‰$.[38] Standardized sample $\delta^{30}Si$ values are calculated from the regression line as:

$$\delta^{30}Si = slope \times \delta^{30}Si_{measured} + intercept \qquad (2)$$

3 Results and discussion

3.1 Nu Sil inlet system

Use of the BTO silicone seal on the sample inlet port is crucial to high accuracy measurements. When samples are heated to 590 °C the original Viton® seals used in the Nu Carb warm sufficiently to release volatile organics that produce peaks in the mass spectrum at m/z 82 through 87, interfering with the SiF_3^+ peaks at m/z 85, 86 and 87. The BTO seal initially produces similar peaks, but they are eliminated after the seal is held at the analytical temperature for a few hours which is easily achieved by running a sample carousel containing several empty sample vials. Individual BTO seals last for a few thousand analyses.

As part of QC/QA procedures, potential interfering masses can be monitored for each analysis by measuring the signal at m/z 83 (one of the larger peaks given off by the BTO seal) with acceptable readings indicated by a peak height that does not exceed background. Deviations in the $\delta^{29}Si : \delta^{30}Si$ ratio also proved to be a sensitive indicator of the presence of interfering masses. The interfering signals biased the $\delta^{29}Si : \delta^{30}Si$ ratio to be more negative than the theoretical value of 0.5110 (ref. 27, 38 and 40) for samples with positive $\delta^{30}Si$ values and to be more positive than expectation for samples with negative $\delta^{30}Si$ values. This issue is essentially eliminated with BTO seals where the average $\delta^{29}Si : \delta^{30}Si$ ratio for Big Batch with its negative $\delta^{30}Si$ value is $+0.5112 \pm 0.0012$ ($1\sigma_{SD}$) while diatomite with its positive $\delta^{30}Si$ value has an average ratio of $+0.5085 \pm 0.0023$ ($1\sigma_{SD}$) (Table 1).

Multiple precautions ensure the final $BaSiF_6$ product is free of both water and HF as water vapor decomposes the analyte gas, SiF_4, and, in a moist environment, HF can react with the borosilicate glass sample vials producing contaminant SiF_4 and H_2O. First, samples are preheated to 110 °C prior to being loaded into the Nu Sil. Then the sample chamber of the Nu Sil is kept at 70 °C to maintain sample dryness, and finally each sample is heated to 250 °C for 20 min under vacuum after being attached to the sample port of the Nu Sil. Although the initial heating to 110 °C should effectively remove HF and water, the additional precautions ensure that the samples remain dry prior to analysis. The Nu Sil carousel holds 50 sample vials, which at our analytical rate of 48 minutes per analysis, requires 40 hours to analyze an entire carousel. Maintaining the Nu Sil sample chamber at 70 °C minimizes absorption of water by samples during this time. Finally, any water that is absorbed while vials are in the Nu Sil sample chamber is eliminated by the prebaking of each sample at 250 °C under vacuum before analysis. The pre-bake does not add to the analysis time (apart from the first sample) as it starts at nearly the same time as does the isotopic analysis of the previous sample and the time required to analyze a sample and then prepare the dual inlet for the next is >20 minutes. The prebake procedure does reduce the time required to achieve the 590 °C sample reaction temperature.

3500 | J. Anal. At. Spectrom., 2025, 40, 3495–3506

This journal is © The Royal Society of Chemistry 2025

Table 1 Summary of results for standards multipoint calibrations. Statistics are means (δ^{29}Si & δ^{30}Si), 95% confidence intervals (95% CI), standard deviations ($1\sigma_{SD}$) and the number of replicates (N)[b]

Standard	$^{29}\delta$Si (‰)	95% CI	$1\sigma_{SD}$	$^{30}\delta$Si (‰)	95% CI	$1\sigma_{SD}$	δ^{29}Si : δ^{30}Si[b]	95% CI	$1\sigma_{SD}$	N	Consensus values, $^{30}\delta$Si (‰)[a]
NBS	+0.010	0.004	0.020	+0.026	0.006	0.032	0.0507	0.0003	0.0020	119	0.000
Diatomite	+0.629	0.004	0.020	+1.236	0.005	0.030	0.5085	0.0004	0.0022	117	+1.260
Big batch	−5.334	0.004	0.030	−10.450	0.007	0.057	0.5112	0.0002	0.0013	226	−10.480
ALOHA$_{1000}$	+0.647	0.012	0.028	+1.274	0.012	0.029	0.5086	0.0005	0.0011	22	+1.240

Multipoint calibration of δ^{30}Si with big batch, NBS and diatomite

	Mean	95% CI	$1\sigma_{SD}$	N
Slope	0.9822	0.0018	0.0040	20
Intercept	−3.192	0.035	0.008	20
R^2	0.99998	0.00001	0.00003	20

[a] Published consensus values for diatomite,[38] Big Batch[38] and Aloha$_{1000}$.[24] [b] δ^{29}Si : δ^{30}Si calculated from data normalized to the reference gas before calibration (eqn (2)).

3.2 Sample preparation chemistry

The lack of Si isotope fractionation is already proven for the precipitation of Cs_2SiF_6 (ref. 27) and for the conversion of Cs_2SiF_6 to $BaSiF_6$.[28] While it is possible to precipitate $BaSiF_6$ directly after the dissolution of SiO_2 in HF, the choice of producing Cs_2SiF_6 as an intermediate product serves to prevent the variable formation of BaF_2 during $BaSiF_6$ precipitation which would void using the mass or volume of the precipitate as an indicator of silicon content during sample loading. Most methods to produce $BaSiF_6$ directly from SiO_2 avoid BaF_2 formation by limiting the addition of BaCl to a small stoichiometric excess (e.g. 1%) over the amount of Si in the presence of excess HF.[28] As the sample precipitation procedure described above begins with samples of SiO_2 of variable weight in the milligram range, achieving a consistent slight excess of Ba becomes problematic. In the recommended procedure, the dissolution of Cs_2SiF_6 produces SiF_6^- ions in the exact stoichiometric proportion required for the quantitative precipitation of all Si as $BaSiF_6$ with no excess HF, facilitating greater flexibility in the amount of barium that can be added while still avoiding the formation of BaF_2. A small excess of HF is provided (~5 micromoles) which is small enough that the BaCl + HF addition avoids BaF_2 formation while aiding in the quantitatively precipitation of $BaSiF_6$.

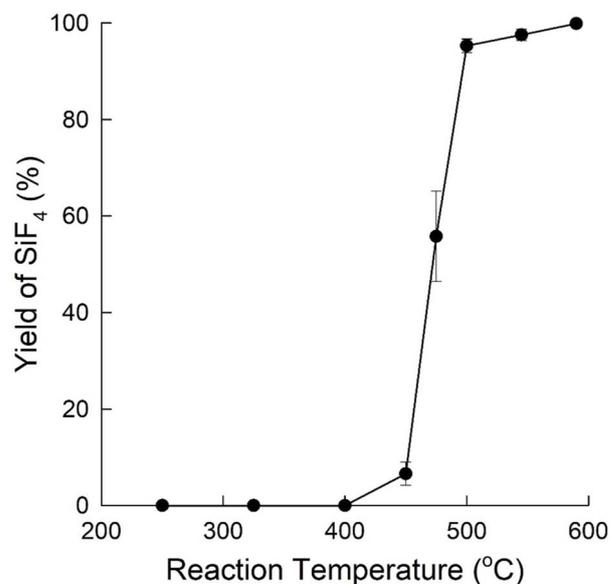### 3.3 Optimizing the thermal decomposition of $BaSiF_6$

The yield of SiF_4 from the thermal decomposition of $BaSiF_6$ is already proven to be quantitative.[28,32] The decomposition of $BaSiF_6$ begins at 300 °C;[41] however, differences in temperature between the location of the feedback thermocouple in the furnace and the $BaSiF_6$ in the sample vial in the center of the furnace requires that an optimum decomposition time and temperature be determined empirically (see SI section S2). A decomposition time of 10 min was deemed a reasonable compromise between the temperature required for complete decomposition and the speed of analysis. Using this heating

time, $BaSiF_6$ decomposition was apparent above 450 °C and rose to 99.8 ± 0.16% ($1\sigma_{SD}$) completion at the chosen decomposition temperature of 590 °C (Fig. 5). The high thermal decomposition temperature also means that the $BaSiF_6$ is stable at the prebake temperature of 250 °C.

3.4 Calibration verification

Si isotope values are routinely reported relative to the standard NBS28 using delta notation. For dual inlet IRMS, this can be achieved by the analysis of NBS28 to determine the difference, δ^{30}Si$_{offset}$, between the standard (assumed to be zero) and the reference gas. The δ^{30}Si of samples is then calculated[39] from

Fig. 5 Yield of SiF_4 from the thermal decomposition of $BaSiF_6$ as a function of thermocouple temperature. Error bars are standard deviations of triplicate measurements at each temperature.

their $\delta^{30}Si$ values measured relative to the reference gas, $\delta^{30}Si_{measured}$, as:

$$\delta^{30}Si = (\delta^{30}Si_{measured} + \delta^{30}Si_{offset})$$
$$+ (\delta^{30}Si_{measured} \times \delta^{30}Si_{offset})/1000 \qquad (3)$$

The approach used wherein differs in that we use a regression approach to calculate $\delta^{30}Si$ from the relationship between $\delta^{30}Si_{measured}$ for a series of standards regressed against their consensus values. The regression approach produces a smaller normalization error than the single-point normalization to NBS28 as it is more robust against random error in the analysis of any one standard.[39] A random selection of 20 calibration curves generated on the Nu Sil gave a mean slope of 0.9822 ± 0.0018 (95% CI) with an average intercept of −3.192 ± 0.035 (95% CI) and a mean R^2 of 0.99998 ± 0.00001 (95% CI) (Table 1). The correlation coefficient of the calibration curve is very close to unity because standards are well calibrated and the systematic error introduced during mass spectrometric analyses is linear within a limited dynamic range.[42] The deviation of the slope from unity is related to the mass bias within the mass spectrometer with the non-zero intercept reflecting the $\delta^{30}Si$ value of the reference gas.[42]

As most $\delta^{30}Si$ values published to date were produced using a single point normalization to NBS28, it is important to evaluate whether that single point calibration and the multipoint calibration recommended here produce significantly different results. In the multipoint regression approach, the value obtained for NBS28 is dictated by the regression rather than being assumed to be zero as done in the single-standard approach. The regression approach for the same 20 calibrations as above predicts a value of NBS28 of +0.025 ± 0.033‰ ($1\sigma_{SD}$) (Table 1) compared to the assumed value of zero, with the difference being within the analytical precision of current $\delta^{30}Si$ measurements.[24,38,43]

The Nu perspective is capable of analyzing samples that are at least two orders of magnitude smaller than recommended here; however, at least two factors make this impractical. First is the difficulty of consistently loading a very small mass of $BaSiF_6$ into a sample vial. Consistency is required so that the reference gas balancing procedure is successful for all samples in a sample carousel as there is a limit to the range of sample sizes that can be balanced at a given gas pressure in the reference bellows. Moreover, SiF_4 has a strong tendency to adsorb onto metal surfaces where it remains even after prolonged pumping under high vacuum. The adsorbed gas does exchange when additional SiF_4 gas is introduced, creating a memory effect for sequential samples. The effect is inconsequential for sample sizes of 25–50 µg Si but would be more pronounced with very small samples. This limitation might be overcome by heating the entire analytical train while analyzing samples, but the challenge of consistently loading extremely small samples remains.

3.5 Precision and accuracy

Maximum precision requires optimizing gas handling during the movement of SiF_4 through the analytical train. This is

illustrated using the expansion or chopping procedure that reduces sample pressure for larger samples as an example. The secondary standard Diatomite was prepared as $BaSiF_6$ and subsamples of a size that would require sample chopping were analyzed using two different times for the evacuation of the space between valve SF and valves SI, SP, SV and SF during the chopping procedure. When the evacuation time was set to 60 s the mean $\delta^{30}Si$ value of chopped samples was 0.58 ± 0.03‰ ($1\sigma_{SD}$) compared to 1.25 ± 0.03‰ ($1\sigma_{SD}$) for an evacuation time of 200 s (Fig. 6). The results for the longer evacuation time align well with those for diatomite samples analyzed using only the microvolume or after expansion (Fig. 6). This result also stresses the importance of adhering to all recommended pumping times associated with sample preparation.

While chopping with an appropriate evacuation time produces quality data, avoiding chopping speeds analysis. Sufficient consistency in mass across samples is achieved with the Wiretrol II® samplers described above with the number of times the sampler is inserted into the $BaSiF_6$ powder serving as a measure of sample packing. It is not necessary to weight each sample precisely. Sample mass can be routinely calculated from the transducer pressure reading for a sample using the ideal gas law and the volume between valves PF and SI of 5.53 mL (factory calibration). In practiced hands the risk of loading a sample too large for the microvolume is extremely rare and typically <2% of samples require expansion or chopping. Unintentional loading
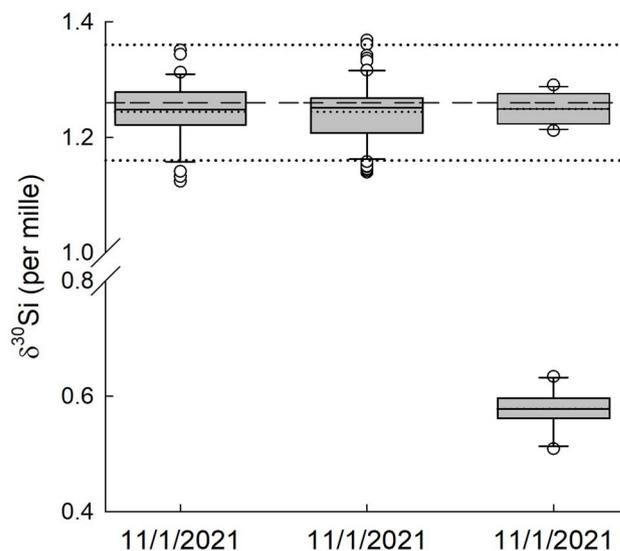

Fig. 6 Whisker plot of the $\delta^{30}Si$ value of diatomite as a function of sample gas analytical volume. Microvolume refers to the volume between valves SF and SM in Fig. 2. Expansion is the volume between valves SI and SM. Chopped refers to discarding the gas between valves Si and SF after expansion as described in the text. Long dashed line is consensus value of +1.26‰ for diatomite with the two long dotted lines reflecting the reported uncertainty of ± 0.10‰ ($1\sigma_{SD}$, Table 1).[38] For the whisker plots the top and bottom of the shaded box indicate the 25th percentile, the solid line within the box marks the median, the dotted line marks the mean and the boundary of the box farthest from zero indicates the 75th percentile. Error bars above and below the box indicate the 90th and 10th percentiles. Symbols are outliers.

of samples that are too small is also extremely rare when using this sample loading method.

The long-term reproducibility for measurements on secondary standards and reference materials made over several months are given in Table 1. Mean δ^{30}Si values for the standards NBS28, Big Batch and diatomite obtained by the thermal decomposition of BaSiF$_6$ are all within 0.03‰ or better relative to their consensus values[38] and the average δ^{30}Si of the reference seawater ALOHA$_{1000}$ (ref. 24) is within 0.034‰ (Table 1) indicating excellent performance of the Nu Sil and Nu perspective. External reproducibility of each of the standards is ≤0.02‰ (95% CI) comparable to the precision obtained by MC-ICPMS.[24,38]

The secondary standard diatomite was used in a more detailed assessment of performance. The consensus value for diatomite, 1.26 ± 0.20 ($2\sigma_{SD}$), is derived from measurements from six laboratories whose results were reported in Reynolds *et al.* (2007).[38] Between 2007 and January 2024, 128 additional studies have reported additional statistics for diatomite, 124 of which were performed on MC-ICP mass spectrometers (Table S8). The mean δ^{30}Si values from each of those studies and the original data from Reynolds *et al.* 2007 (ref. 38) are plotted as a histogram along with the corresponding probability density function (PDF) in Fig. 7a. The PDF is unimodal with a strong peak at +1.238‰ representing the mode of the PDF. The overall mean of the measurements is +1.248 ± 0.109‰ ($2\sigma_{SD}$, $n = 137$). Those values differ from the mean for diatomite from the Nu Sil (+1.236 ± 0.060‰, $2\sigma_{SD}$, $n = 117$) by 0.002‰ for the PDF peak and by 0.012‰ for the overall mean of measurements. A similar analysis for measurement uncertainty ($2\sigma_{SD}$) reported in these same studies reveals a PDF that is also unimodal but skewed to the right (Fig. 7b) with a mode of 0.095‰. The mean $2\sigma_{SD}$ across studies is 0.14‰ compared to the uncertainty in the current consensus value for diatomite of 0.20‰ (Fig. 7b). The average
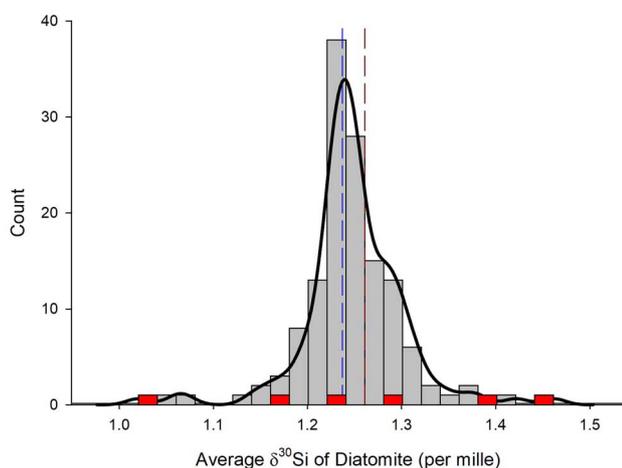
$2\sigma_{SD}$ obtained using the Nu Sil (0.060‰, Table S2) is lower than that for all but seven studies (5.1%) with the PDF predicting that 10.7% of studies would have a lower value for $2\sigma_{SD}$. The reported level of precision for measurements on the Nu Sil can be routinely obtained with quadruplicate analyses of samples with each replicate analyzed within a separate carousel of samples.

Several types of previously analyzed materials were obtained and analyzed for their silicon isotopic composition to illustrate the versatility of the sample preparation chemistry and that capabilities of the Nu Sil. The materials range from dissolved Si in rivers and oceans, soils, clays and sponge spicules representing a wide range of sample composition and matrices. The method is designed to systematically eliminate potential matrix interferences by converting all samples to SiO$_2$ prior to their conversion to BaSiF$_6$. The results show excellent agreement with published values for all of these materials (Table 2), indicating that the method is indeed insensitive to sample matrix effects. With the exception of the one river water sample measurements from the Nu Sil agree with previously published results to within 0.08‰ or better (range 0‰ to 0.08‰, mean absolute difference 0.05 ± 0.06‰, $n = 11$) irrespective of material type. We note that the results in Table 1 for the standards NBS28 (RM8546, a quartz), Big Batch (cristobalite) and diatomite (calcined diatomite) add to the range of material types successfully analyzed.

3.6 Sample size

Analytical precision is consistent for BaSiF$_6$ masses from ~10 to ~60 micrograms of Si (Fig. 8). However, it is impractical to analyze samples across this entire mass range within a single analytical run as maximum accuracy relies on the dual inlet system being able to balance the pressure of the sample and reference gases in the ionization source. The minimum pressure of SiF$_4$ within the reference bellows that is sufficient to balance larger samples is too high to effectively balance the lower pressure associated with very small samples. The problem is easily solved by analyzing samples and standards of similar mass within a given analytical run.

3.7 Memory effects

A memory effect is apparent when the isotope values of sequentially analyzed samples differ by several per mille. For example, when Big Batch (δ^{30}Si = −10.48‰) is run before two replicates of diatomite (+1.26‰) the δ^{30}Si value of the first diatomite is ~25% percent too negative while the second is unaffected. The memory effect is likely related to the tendency for SiF$_4$ gas to adhere to metal surfaces and could possibly be reduced by heating the entire analytical train w memory impacts are captured through the recommendation that replicate samples be analyzed in separate analytical runs which varies the identity of adjacent samples across replicates. For natural materials where the difference in δ^{30}Si among samples is typically 3‰ or less, the maximum memory effect without such precautions is 0.03‰ which is within analytical uncertainty. When a sample is known to have a δ^{30}Si value well outside of this range (such as Big Batch) it should be run in

Fig. 7 (A) Histogram of mean δ^{30}Si values for diatomite reported in the literature including and following[38] through January 2025. Red bars are the original data from[38] used to define the current consensus value for this material. Black line is the probability density function. Vertical dashed lines are the average from[38] (dark red) and from the Nu Sil (blue). (B) As in A but for the uncertainty in the mean isotope value for diatomite ($2\sigma_{SD}$) reported in each study.

This journal is © The Royal Society of Chemistry 2025

J. Anal. At. Spectrom., 2025, **40**, 3495–3506 | **3503**

Table 2 Comparison of $\delta^{30}Si$ values for a variety of natural materials measured using multi-collector ICP-MS and by the thermal decomposition of BaSiF$_6$ on the Nu Sil

Sample type	Station or sample ID	Silicic acid (μM Si)	$^{30}\delta Si$ (‰) MC-ICP-MS	$1\sigma_{SD}$	N	$\delta^{30}Si$ (‰) Nu-Sil	$1\sigma_{SD}$	N
River water[44]	Mungo	324	+0.91	NA	1	+1.1	NA	1
Seawater silicic acid[a]	GEOTRACES 11667	39.9	+1.66[b]	0.01	2	+1.66	0.01	3
	GEOTRACES 11915	29.7	+1.71[b]	0.06	2	+1.71	0.09	3
	ALOHA1000	112.8	+1.24[g]	0.10	11	+1.29	0.01	44
Soils[f]	GBW-07401	62.60	−0.27	0.03	78	−0.22		
	GBW-07404	50.95	−0.76	0.06	79	−0.84		
	GBW-07407	32.67	−1.82	0.09	72	−1.62		
Clay minerals		Wgt% SiO$_2$						
	Kaolinite[d]	46.55	−2.16[c]	0.08	15	−2.13	0.06	7
	Calcined Kaolinite[e]	46.55	−1.44[c]	0.09	16	−1.43	0.06	6
Marine sponge spicules[h]	*Vazella pourtalesi*	Depth (m)						
	B0027	199	−1.61	0.07	nr	−1.65	0.08	12
	B0044	199	−1.73	0.06	nr	−1.75	0.05	12
	B0227	206	−1.75	0.06	nr	−1.71	0.06	12

[a] Seawater samples from the Arctic Ocean. Numbers are sample number form the GEOTRACES cruise GN01.[45] [b] NuPlasma 1700 at IGMR ETH Zürich, Switzerland. [c] Analyses at Bristol, UK *via* Thermo-Fisher Neptune MC-ICPMS by Kate Hendry and Jade Hatton. [d] Source: Texas, USA. [e] Source: Natural Pigments, LLC, USA. [f] Original measurements reported in Delvigne *et al.* (2021).[46] [g] Mean from 11 laboratories with 3–10 independent replicates each.[24] [h] Further details published in Hendry *et al.* (2019)[47] data available at **https://doi.pangea.de/10.1594/PANGEA.898676**.
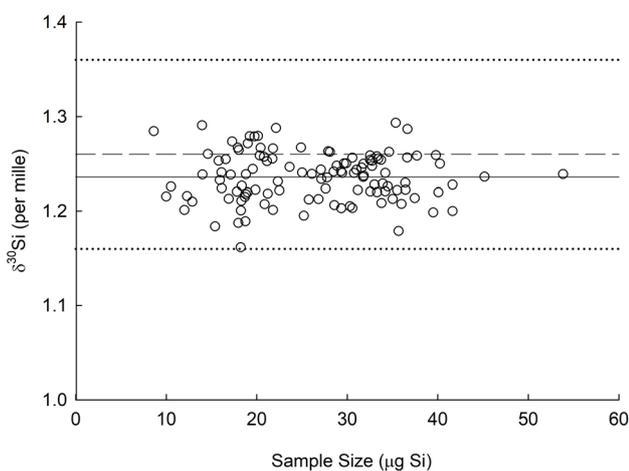
Fig. 8 $\delta^{30}Si$ value of diatomite as a function of sample size expressed as micrograms of Si for a typical source tuning. Horizontal dashed line is the consensus $\delta^{30}Si$ value for diatomite of +1.26‰ with the dotted lines representing the reported uncertainty of the consensus value, ± 0.10‰ ($1\sigma_{SD}$, Table 1).[38] Horizontal solid line is the mean for the samples.

duplicate or triplicate in adjacent positions in the sample carousel followed by a sacrificial material (diatomite works well) whose $\delta^{30}Si$ value is aligned with those expected for subsequent samples. The initial replicate of the sample and the sacrificial material are subject to the full memory effect eliminating the issue for subsequent replicates and samples.

4   Summary

The precision of the $\delta^{30}Si$ measurement obtained through the automated thermal decomposition of BaSiF$_6$ using the Nu Sil is

excellent and is comparable to the best that is achieved with current MC-ICPMS methods. Si isotope analysis with the combination of the Nu Sil and Nu perspective IRMS is fully automated allowing unattended sample processing. Daily instrument tuning typically is rarely required, and when necessary, requires only minutes. The recommended sample preparatory chemistry is straightforward and is applicable to a wide variety of solid and aqueous natural materials. Analytical throughput is 30 analyses daily allowing for the relatively rapid processing of large sample sets.

Author contributions

MAB: conceptualization, project administration, funding acquisition, supervision, methodology, formal analysis, writing – original draft. SFR: conceptualization, investigation, methodology, software, validation, writing – review & editing. JLJ: data curation, formal analysis, methodology, validation, writing – review & editing. IC: formal analysis investigation methodology, validation, writing – review & editing. JTM: formal analysis investigation methodology, validation, writing – review & editing.

Conflicts of interest

Stephen F. Rablen is an employee of Nu Instruments Ltd, Leicester, UK that manufactures the Nu Sil and Nu perspective.

Data availability

The data supporting this article have been included as part of the supplementary information (SI). Supplementary information is available. See DOI: **https://doi.org/10.1039/d5ja00294j**.

3504 | *J. Anal. At. Spectrom.*, 2025, **40**, 3495–3506

This journal is © The Royal Society of Chemistry 2025

Acknowledgements

References

1 K. J. R. Rosman and P. D. P. Taylor, *Pure Appl. Chem.*, 1998, **70**, 217–236.

2 T. P. Ding, G. R. Ma, M. X. Shui, D. F. Wan and R. H. Li, *Chem. Geol.*, 2005, **218**, 41–50.

3 T. P. Ding, J. X. Zhou, D. F. Wan, Z. Y. Chen, C. Y. Wang and F. Zhang, *Geochim. Cosmochim. Acta*, 2008, **72**, 1381–1395.

4 C. L. De La Rocha, M. A. Brzezinski and M. J. DeNiro, *Geochim. Cosmochim. Acta*, 1997, **61**, 5051–5056.

5 D. A. Frick, R. Remus, M. Sommer, J. Augustin, D. Kaczorek and F. von Blanckenburg, *Biogeosciences*, 2020, **17**, 6475–6490.

6 K. Doering, C. Ehlert, K. Pahnke, M. Frank, R. Schneider and P. Grasse, *Front. Mar. Sci.*, 2021, **8**, 1–17.

7 K. R. Hendry, H. Pryer, S. L. Bates, F. Mienis and J. R. Xavier, *Geochemical Perspective Letters*, 2024, **30**, 57–63.

8 T. Ding, C. Wang, F. Zhang and D. Wan, *Chin. Sci. Bull.*, 1998, **43**, 33.

9 R. M. G. Armytage, R. B. Georg, P. S. Savage, H. M. Williams and A. N. Halliday, *Geochim. Cosmochim. Acta*, 2011, **75**, 3662–3676.

10 S. Epstein and H. P. J. Taylor, *Proceedings of the Second Lunar Science Conference*, 1971, vol. 2, 1421–1441.

11 H. P. J. Taylor and S. Epstein, *Earth Planet. Sci. Lett.*, 1970, **9**, 208–210.

12 I. J. Onyett, M. Schiller, G. V. Makhatadze, Z. Deng, A. Johansen and M. Bizzarro, *Nature*, 2023, **619**, 539–544.

13 R. A. Mendybaev, M. Kamibayashi, F. Z. Teng, P. S. Savage, R. B. Georg, F. M. Richter and S. Tachibana, *Geochim. Cosmochim. Acta*, 2021, **292**, 557–576.

14 R. Tanaka, C. Potiszil and E. Nakamura, *Planet. Sci. J.*, 2021, **102**, 12.

15 C. B. Douthitt, *Geochim. Cosmochim. Acta*, 1982, **46**, 1449–1458.

16 C. L. De La Rocha, M. A. Brzezinski, M. J. DeNiro and A. Shemesh, *Nature*, 1998, **395**, 680–683.

17 R. B. Georg, B. C. Reynolds, M. Frank and A. N. Halliday, *Earth Planet. Sci. Lett.*, 2006, **249**, 290–306.

18 S. Opfergelt and P. Delmelle, *C. R. Geosci.*, 2012, **344**, 723–738.

19 K. E. Giesbrecht, D. E. Varela, G. F. de Souza and C. Maden, *Global Biogeochem. Cycles*, 2022, **36**, e2021GB007107.

20 Q. Zhang, L. Zhao, D. Zhou, A. P. Nutman, R. N. Mitchell, Y. Liu, Q.-L. Li, H.-M. Yu, B. Fan, C. J. Spencer and X.-H. Li, *Sci. Adv.*, 2023, **9**, eadf0693.

21 X. Y. Chen, H. S. Chafetz and T. J. Lapen, *Geochim. Cosmochim. Acta*, 2020, **283**, 184–200.

22 Q. C. Cui, X. W. Liu, Z. Y. Wang, W. D. Sun, Y. Y. Xiao and X. L. Sun, *Global Biogeochem. Cycles*, 2024, **38**, e2023GB007894.

23 T. Ding, S. Jiang, Y. Li, J. Gao and B. Hu, *Geochemistry of Silicon Isotopes*, 2017.

24 P. Grasse, M. A. Brzezinski, D. Cardinal, G. F. de Souza, P. Andersson, I. Closset, Z. M. Cao, M. H. Dai, C. Ehlert, N. Estrade, R. Francois, M. Frank, G. B. Jiang, J. L. Jones, E. Kooijman, Q. Liu, D. W. Lu, K. Pahnke, E. Ponzevera, M. Schmitt, X. Sun, J. N. Sutton, F. Thil, D. Weis, F. Wetzel, A. Zhang, J. Zhang and Z. L. Zhang, *J. Anal. At. Spectrom.*, 2017, **32**, 562–578.

25 C. L. De La Rocha, M. A. Brzezinski and M. J. DeNiro, *Anal. Chem.*, 1996, **68**, 3746–3750.

26 T. Ding, S. Jiang, D. Wan, Y. Li, J. Li, H. Song, Z. Liu and X. Yao, *Silicon Isotope Geochemistry*, Geological Publilshing House, Beijing, 1996.

27 M. A. Brzezinski, J. L. Jones, C. P. Beucher and M. S. Demarest, *Anal. Chem.*, 2006, **78**, 6109–6114.

28 P. De Bievre, G. Lenaers, T. J. Murphy, H. S. Peiser and S. Valkiers, *Metrologia*, 1995, **32**, 103–110.

29 B. Andreas, Y. Azuma, G. Bartl, P. Becker, H. Bettin, M. Borys, I. Busch, P. Fuchs, K. Fujii, H. Fujimoto, E. Kessler, M. Krumrey, U. Kuetgens, N. Kuramoto, G. Mana, E. Massa, S. Mizushima, A. Nicolaus, A. Picard, A. Pramann, O. Rienitz, D. Schiel, S. Valkiers, A. Waseda and S. Zakel, *Metrologia*, 2011, **48**, S1.

30 M. J. Leng and H. J. Sloane, *J. Quat. Sci.*, 2008, **23**, 313–319.

31 J. H. Reynolds and J. Verhoogen, *Geochim. Cosmochim. Acta*, 1953, **3**, 224–234.

32 D. Tilles, *J. Geophys. Res.*, 1961, **66**, 3003–3013.

33 S. Valkiers, K. Rube, P. Taylor, T. DIng and M. Inkret, *Int. J. Mass Spectrom.*, 2005, **242**, 321–323.

34 S. Valkiers, G. Mana, K. Fujii and P. Becker, *Metrologia*, 2011, **48**, S26–S31.

35 D. Tiping, in *Handbook of Stable Isotope Analytical Techniques*, ed. P. A. De Groot, Elsevier, New York, 2004, vol. 1, pp. 523–537.

36 R. B. Georg, B. C. Reynolds, M. Frank and A. N. Halliday, *Chem. Geol.*, 2006, **235**, 95–104.

37 D. M. Nelson and J. J. Goering, *Anal. Biochem.*, 1977, **78**, 139–147.

38 B. C. Reynolds, J. Aggarwal, L. Andre, D. Baxter, C. Beucher, M. A. Brzezinski, E. Engström, R. B. Georg, M. Land, M. J. Leng, S. Opfergelt, I. Rodushkin, H. J. Sloane, S. H. J. M. Van den Boorn, P. Z. Vroon and D. Cardinal, *J. Anal. At. Spectrom.*, 2007, **22**, 561–568.

39 D. Paul, G. Skrzypek and I. Fórizs, *Rapid Commun. Mass Spectrom.*, 2007, **21**, 3006–3014.

40 E. D. Young, A. Galy and H. Nagahara, *Geochim. Cosmochim. Acta*, 2002, **66**, 1095–1104.

41 J. R. Rumble, in *CRC Handbook of Chemistry and Physics (Internet Edition 2019)*, CRC Press/Taylor & Francis, Boca Raton, FL, 75 edn, 2019.

42 S. T. Nelson, *Rapid Commun. Mass Spectrom.*, 2000, **14**, 1044–1046.

This journal is © The Royal Society of Chemistry 2025

J. Anal. At. Spectrom., 2025, **40**, 3495–3506 | **3505**

43 B. C. Reynolds, R. B. Georg, F. Oberli, U. Wiechert and A. N. Halliday, *J. Anal. At. Spectrom.*, 2006, **21**, 266–269.

44 S. Opfergelt, G. de Bournonville, D. Cardinal, L. André, S. Delstanche and B. Delvaux, *Geochim. Cosmochim. Acta*, 2009, **73**, 7226–7240.

45 M. A. Brzezinski, D. E. Varela, B. D. Jenkins, K. N. Buck, S. M. Kafrissen and J. L. Jones, *Elementa: Science of the Anthropocene*, 2022, **10**, 00087.

46 C. Delvigne, A. Guihou, J. A. Schuessler, P. Savage, F. Poitrasson, S. Fischer, J. E. Hatton, K. R. Hendry, G. Bayon, E. Ponzevera, B. Georg, A. Akerman, O. S. Pokrovsky, J.-D. Meunier, P. Deschamps and I. Basile-Doelsch, *Geostand. Geoanal. Res.*, 2021, **45**, 525–538.

47 K. R. Hendry, L. Cassarino, S. L. Bates, T. Culwick, M. Frost, C. Goodwin and K. L. Howell, *Quat. Sci. Rev.*, 2019, **210**, 1–14.